

Article

Radvaniceite, GeS_2 , a New Germanium Sulphide, from the Kateřina Mine, Radvanice near Trutnov, Czech Republic

Jiří Sejkora ^{1,*}, Vladimír Žáček ², Radek Škoda ³ , František Laufek ² and Zdeněk Dolníček ¹

¹ Department of Mineralogy and Petrology, National Museum, Cirkusová 1740, 193 00 Prague 9—Horní Počernice, Czech Republic; zdenek.dolnicek@nm.cz

² Czech Geological Survey, Klárov 3, 118 21 Prague 1, Czech Republic; vladimir.zacek@geology.cz (V.Ž.); frantisek.laufek@geology.cz (F.L.)

³ Department of Geological Sciences, Faculty of Science, Masaryk University, Kotlářská 2, 611 37 Brno, Czech Republic; rskoda@sci.muni.cz

* Correspondence: jiri.sejkora@nm.cz

Abstract: The new mineral radvaniceite, GeS_2 , was found on the burning coal mine dump of the abandoned Kateřina coal mine at Radvanice, near Trutnov, northern Bohemia, Czech Republic. It occurs as aggregates resembling cotton tufts up to 5 mm in size; they are composed of acicular crystals up to fibres about 1–5 μm thick and up to 3 mm in length. Individual fibres are distorted and partly resemble bent wires nucleated on rock fragments or on black, crumbly ash, in association with minerals of solid solutions of Bi-Sb and stangersite, herzenbergite, and greenockite. Radvaniceite was also observed as irregular grains in a range of 10–50 μm in size, forming part of earlier multicomponent aggregates upon which the above-described crystals grow. These aggregates are formed, in addition to radvaniceite, by minerals of Bi-Sb, Bi_2S_3 - Sb_2S_3 and Bi_2S_3 - Bi_2Se_3 solid solutions, Bi_3S_2 , Bi-sulpho/seleno/tellurides, tellurium, unnamed PbGeS_3 , Cd_4GeS_6 , GeAsS , $\text{Sn}_5\text{Sb}_3\text{S}_7$, stangersite, greenockite, cadmoindite, herzenbergite, teallite, and Sn- and/or Se-bearing galena. Radvaniceite is formed under reducing conditions by direct crystallization from hot gasses (250–350 °C) containing Cl and F at a depth of 30–60 cm under the surface of a burning coal mine dump; the mine dump fire started spontaneously, and no anthropogenic material was deposited there. Acicular crystals up to fibres of radvaniceite are elastic to flexible; are white to yellowish grey in colour, with white streaks; are translucent in transmitted light; and have vitreous to adamantine lustre. Cleavage and fracture were not observed. The calculated density is 3.05 and 2.99 $\text{g}\cdot\text{cm}^{-3}$ for the empirical and ideal formulae, respectively. Radvaniceite is transparent under the microscope, with a very weak pleochroism (from colourless to pale greenish yellow), and has a refraction index > 1.8. Under reflected light, radvaniceite is light grey; bireflectance and pleochroism were not observed due to abundant, white to grey, internal reflections. Anisotropy in crossed polars is distinct with grey rotation tints. Reflectance values of radvaniceite in air ($R_{\text{min}}-R_{\text{max}}$, %) are: 15.4–18.8 at 470 nm, 16.1–20.4 at 546 nm, 16.4–20.8 at 589 nm, and 16.9–20.9 at 650 nm. The empirical formula, based on electron-microprobe analyses, is $(\text{Ge}_{0.99}\text{Bi}_{0.01})_{\Sigma 1.00}(\text{S}_{1.97}\text{Se}_{0.03})_{\Sigma 2.00}$. The ideal formula is GeS_2 , which requires Ge 53.10, S 46.90, total 100 wt. %. Radvaniceite is monoclinic, Pc , $a = 6.8831(12)$, $b = 22.501(3)$, $c = 6.8081(11)$ Å, $\beta = 120.365(9)^\circ$, with $V = 909.8(4)$ Å³ and $Z = 12$. The strongest reflections of the powder X-ray diffraction pattern [d , Å (I) (hkl)] are: 5.7395 (100) (11-1, 110), 5.2067 (16) (021), 3.3650 (33) (111, 11-2), 2.8417 (33) (022), 2.8236 (16) (170, 17-1), 2.8134 (20) (080) and 2.6257 (19) (240, 24-2). According to X-ray powder diffraction data and Raman spectroscopy, radvaniceite is a natural analogue of synthetic monoclinic low-temperature β - GeS_2 with distorted GeS_4 tetrahedra forming four corner-sharing tetrahedral chains, which are connected by corner-sharing tetrahedra in a three-dimensional structure. We named the mineral after its type locality, Radvanice, one of the past centres of coal mining in the Czech limb of the Intra-Sudetic Basin. This mineral and its name have been approved by the Commission on New Minerals, Nomenclature and Classification of the International Mineralogical Association (number 2021-052).

Keywords: radvaniceite; new mineral; germanium sulphide; Raman spectroscopy; Radvanice; Czech Republic



Citation: Sejkora, J.; Žáček, V.; Škoda, R.; Laufek, F.; Dolníček, Z. Radvaniceite, GeS_2 , a New Germanium Sulphide, from the Kateřina Mine, Radvanice near Trutnov, Czech Republic. *Minerals* **2022**, *12*, 222. <https://doi.org/10.3390/min12020222>

Academic Editors: Irina O. Galuskina, Igor V. Pekov and Luca Bindi

Received: 18 January 2022

Accepted: 6 February 2022

Published: 9 February 2022

Publisher's Note: MDPI stays neutral with regard to jurisdictional claims in published maps and institutional affiliations.



Copyright: © 2022 by the authors. Licensee MDPI, Basel, Switzerland. This article is an open access article distributed under the terms and conditions of the Creative Commons Attribution (CC BY) license (<https://creativecommons.org/licenses/by/4.0/>).

1. Introduction

Synthetic GeS₂ phases were known long before they were found in natural conditions, and were studied due their interesting electronic and optical properties [1]. Four crystalline modifications of GeS₂ are known: the first is a high-temperature (stable to 850 °C) α-GeS₂ modification, which crystallises in the monoclinic space group *P2₁/c* [2–4]. The second is a low-temperature β-GeS₂ modification [5], which crystallises in the monoclinic space group *Pc* [6]. It was previously described with orthorhombic symmetry and space group *Fdd2* [7,8]. The transformation between α-GeS₂ and β-GeS₂ occurs at 497 °C at high sulphur activity, or at 520 °C if associated with GeS [5,9]. The other two modifications occur in high-pressure/high-temperature conditions: tetragonal γ-GeS₂ with space group *I-42d* [10] and tetragonal δ-GeS₂ with space group *I4₁/acd* [11], the latter was also prepared in aqueous solution by mild sol ± gel process [1]. It should be noted that, in this paper, we use the notation α-GeS₂ for the high-temperature modification of the GeS₂ phase with *P2₁/c* symmetry and β-GeS₂ for the low-temperature modification showing *Pc* symmetry, as this notation is in agreement with the original work of Dittmar and Schäfer [3], and subsequently MacLachlan et al. [1].

Contrary to the aforementioned studies, Bletskan [5] used a different notation, where α and β suffixes for GeS₂ are interchanged. Although the β-GeS₂ phase (i.e., the analogue of radvaniceite) represents the low-temperature phase, and similar phases stable at standard conditions are commonly referred as α, we keep the original notation.

The first find of the unnamed β-GeS₂ in natural conditions was described from burning waste piles in eastern Pennsylvania (locality Forestville), where the mineral occurs as small tufts (up to 1 mm) of radiating white fibres, probably formed by the vapor–liquid–solid growth mechanism [12,13]. The results of a more detailed study of this mineral phase have not yet been published. The first descriptions of radvaniceite (as an unnamed GeS₂) from the burning mine dump of the Kateřina mine, at Radvanice, near Trutnov (Czech Republic), were given by Sejkora et al. [14] and Sejkora [15]. At the time of their publication, the strict rules of the International Mineralogical Association Commission on New Minerals and Mineral Names [16] did not allow submission of this natural phase as a valid mineral species: “It has therefore been decided that, as a general rule, products of combustion are not to be considered as minerals in the future”. However, the recent change of rules (see CNMNC-IMA proposal 16-F: “Crystal phases forming on the burning coal-dumps with no human agency initiating the fire and no anthropogenic material deposited there should be treated as minerals.” [17]) allows the proposal of this new mineral. Radvaniceite is named after its type locality Radvanice, one of the past centres of coal mining in the Czech limb of the Intra-Sudetic Basin, and a unique locality worldwide with respect to the number and quantity of metal- and metalloid-bearing sublimates [14,15,18–21]. The new mineral and its name have been approved by the Commission on New Minerals, Nomenclature and Classification of the International Mineralogical Association (number 2021-052). The holotype specimen of radvaniceite is deposited in the collections of the Department of Mineralogy and Petrology, National Museum, in Prague, Cirkusová 1740, 19 300 Praha 9, Czech Republic, under the catalogue number P1P 9/2021.

2. Occurrence

Radvaniceite samples were collected from 1995 to 1998 in the central part of a burning coal mine dump in the abandoned Kateřina coal mine (GPS: 50°33′39.0″ N 16°03′56.2″ E), which is situated in the eastern part of the Radvanice village, about 12 km east of the district town of Trutnov (northern Bohemia, Czech Republic). At this mine dump, mine wastes from the former Kateřina mine were deposited for over 100 years; their total volume was estimated to be 2.331 million m³ [22]. In the past, coal was only hand-picked there, and therefore dump material contained 19 vol.% coal on average, and locally up to 40 vol.% [22,23]. Later, during uranium mining at the Kateřina mine, all low-uranium material, including coal and coal-bearing claystones (locally rich in pyrite and base element sulphides) were deposited in this mine dump. The mine dump fire started spontaneously before 1967 and

culminated between 1980 and 1981 [22]. Temperatures in this burning dump reached up to 1000 °C or more. Due to possible ecological hazards for the Radvanice village, the Czech government decided to conduct disposal and remediation operations in this mine dump. The restoration works started in 1998 and were successfully completed in 2005 [22,23].

In the Kateřina mine area, six coal measures are known; thickness of the exploited measures reached ~1 m, exceptionally up to 1.5–1.9 m. The coal-bearing sediments belong to the upper part of the Odolov Member (Stephanian B) of the Czech limb of the Intra-Sudetic Basin which comprises sediments from the Early Mississippian (Namurian C) up to the Early Triassic age [24]. The characteristic feature of the Radvanice coals and surrounding sediments is their mineralization and enrichment in Se, Mo, As, Pb, Cu, Zn, Ge, U, Cd, Sb, Bi, and other elements [25–27]. The increased content of some elements in coal-bearing sediments have been studied since 1945. In addition to experiments with copper and germanium extraction, the uranium mineralization (uraninite and coffinite) was mined from 1952 to 1957. After 1957, only coal was mined, and in 1993 all mines in the Radvanice area were closed.

Radvaniceite was found on a part of the mine dump within an area of 2 m² and about 30–60 cm under the surface. The temperature of mine dump material reached up to 300 °C at this site. Massive crusts, reaching a thickness of about 1–5 cm in places, and formed by sal ammoniac, cryptohalite, and bararite, as well as sulphur and dark red amorphous As-rich sulphur, were developed above the horizon with germanium-bearing mineral phases. Two types of radvaniceite were observed in the studied material. The first comprised rich groups of fibres in association with stangersite [20], herzenbergite, greenockite, and members of Bi-Sb solid solutions. The second type represents irregular radvaniceite grains in the earlier multicomponent aggregates on which the above described fibres grow. In addition to radvaniceite, these aggregates were formed by minerals of Bi-Sb, Bi₂S₃-Sb₂S₃ and Bi₂S₃-Bi₂Se₃ solid solutions, Bi₃S₂, Bi-sulpho/seleno/tellurides, tellurium, unnamed PbGeS₃, Cd₄GeS₆, GeAsS, Sn₅Sb₃S₇, stangersite, greenockite, cadmoindite, herzenbergite, teallite, and Sn- and/or Se-bearing galena. Radvaniceite formed under reducing conditions by direct crystallization from hot gases (250–350 °C) containing Cl and F at depths of 30–60 cm under the surface of a burning coal mine dump.

3. Physical and Optical Properties

As mentioned above, two morphological types of radvaniceite were observed in the studied material. The first type is represented by aggregates resembling cotton tufts up to 5 mm in size (Figure 1); they are composed of acicular crystals up to fibres about 1–5 µm thick and up to 3 mm in length. Individual fibres are distorted and partly resemble bent wires (Figure 2). The second type forms irregular grains 10–50 µm in size as a part of previously formed multicomponent aggregates. Radvaniceite is white to yellowish grey in colour, with white streaks. The mineral is translucent in transmitted light and has vitreous to adamantine lustre. Cleavage and fracture were not observed, the tenacity is elastic to flexible. The calculated density ($Z = 12$) is 3.05 and 2.99 g·cm⁻³ for empirical and ideal formulae, respectively. Radvaniceite is transparent under a microscope, with a very weak pleochroism (from colourless to pale greenish yellow). The index of refraction is >1.8; other properties cannot be determined due to fine nature of the sample.

In reflected light radvaniceite is light grey; bireflectance and pleochroism were not observed due to abundant white to grey internal reflections. Anisotropy in crossed polars is distinct, with grey rotation tints. Reflectance percentages (air) for the four COM wavelengths (R_{\min} and R_{\max} , %) for radvaniceite are: 15.4–18.8 (470 nm), 16.1–20.4 (546 nm), 16.4–20.8 (589 nm), and 6.9–20.9 (650 nm). The full set of reflectance values (spectrophotometer MSP400 Tidas coupled to a Leica microscope, objective 100×, WTiC standard Zeiss 370 in air) are given in Table 1 and plotted in Figure 3.



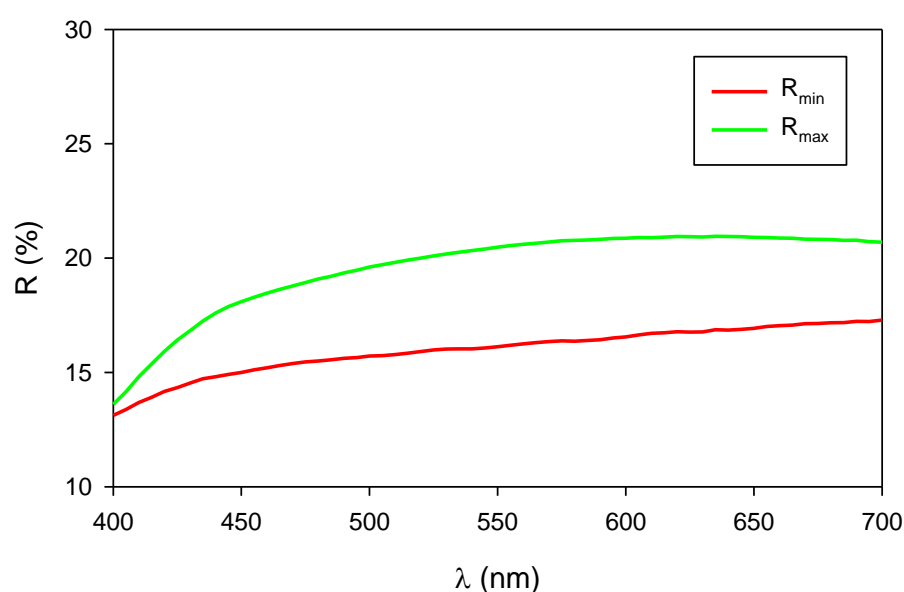
Figure 1. White radvaniceite fibres formed cotton-like aggregates in association with orange stangerite crystals; locality, Radvanice; field of view, 5 mm; photo, J. Sejkora.



Figure 2. Bent fibres of radvaniceite; Radvanice, SEM photo, J. Sejkora.

Table 1. Reflectance values of radvaniceite (measured in air).

R_{\max}	R_{\min}	λ (nm)	R_{\max}	R_{\min}	λ (nm)
13.6	13.1	400	20.6	16.2	560
15.9	14.2	420	20.8	16.4	580
17.6	14.8	440	20.8	16.4	589 (COM)
18.5	15.2	460	20.9	16.6	600
18.8	15.4	470 (COM)	20.9	16.8	620
19.1	15.5	480	20.9	16.9	640
19.6	15.7	500	20.9	16.9	650 (COM)
20.0	15.9	520	20.9	17.0	660
20.3	16.0	540	20.8	17.2	680
20.4	16.1	546 (COM)	20.7	17.3	700

**Figure 3.** Reflectivity curves for radvaniceite.

4. Chemical Composition

The holotype sample of radvaniceite was analysed using a JEOL Superprobe 733 electron microprobe operated in the wavelength-dispersive mode with an accelerating voltage of 20 kV, a specimen current of 20 nA, and a beam diameter of 1–2 μm . The following lines and standards were used: $K\alpha$: chalcopyrite (Fe, S); $L\alpha$: Bi (Bi), CdS (Cd), Cu_3AsS_4 (As), Ge (Ge), Sb_2Se_3 (Sb, Se), Sn (Sn); $M\alpha$: PbS (Pb). The raw intensities were converted into concentrations automatically, using the online ZAF correction program supplied by JEOL. Detection limits were close to 0.02–0.05 wt. %. Absence of H_2O and CO_2 was confirmed by Raman spectroscopy. Chemical analyses of other samples were performed using a Cameca SX100 electron microprobe operating in wavelength-dispersive mode (15 kV, 10 nA, and 0.7 μm wide beam). The following standards and X-ray lines were used to minimise line overlaps: Ge ($\text{Ge}L\alpha$), Bi ($\text{Bi}M\beta$), CdTe ($\text{Cd}L\alpha$), FeS_2 ($\text{Fe}K\alpha$, $\text{SK}\alpha$), NiAs ($\text{As}L\beta$), PbS ($\text{Pb}M\alpha$), PbSe ($\text{Se}L\beta$), PbTe ($\text{Te}L\alpha$), and Sb_2S_3 ($\text{Sb}L\alpha$). Peak counting times were 20 s for all elements, and one half of the peak time for each background. Some elements, such as Cd, Fe, As, Pb, Te, and Sb, were found to be below the detection limits (0.02–0.05 wt. %). Raw intensities were converted to the concentrations of elements using the automatic “PAP” [28] matrix-correction procedure.

Chemical composition of radvaniceite from the holotype sample (Table 2) corresponds to the ideal formula GeS_2 with only minor contents of Sn, Sb, As, and Bi up to 0.01 *apfu*, and Pb up to 0.003 *apfu*, respectively. The extent of Se_{S_1} substitution in anions of this sample is limited to 0.06 *apfu* Se (Figure 4). The empirical formula calculated from the mean of

12 point analyses on the basis of 3 *apfu* is as follows: $(\text{Ge}_{0.99}\text{Bi}_{0.01})_{\Sigma 1.00}(\text{S}_{1.97}\text{Se}_{0.03})_{\Sigma 2.00}$. The ideal formula, GeS_2 , requires Ge 53.10, S 46.90, total 100 wt. %. The representative analyses for the holotype and other samples are given in Table 3. The selenium contents of other samples were detected in the range 0.09–0.10 *apfu* (Figure 4).

Table 2. Chemical data (in wt. %) for the holotype sample of radvaniceite.

Constituent	Mean	Range	Stand. Dev. (σ)	Reference Material
Ge	51.84	50.82–52.80	0.54	Ge
Pb	0.18	0.00–0.45	0.15	PbS
Sn	0.21	0.00–1.23	0.39	Sn
Bi	0.66	0.20–1.00	0.21	Bi
Sb	0.12	0.00–0.56	0.17	Sb_2Se_3
As	0.12	0.00–0.38	0.15	Cu_3AsS_4
S	45.65	44.42–46.66	0.68	chalcopyrite
Se	1.74	0.49–3.42	0.91	Sb_2Se_3
total	100.52			

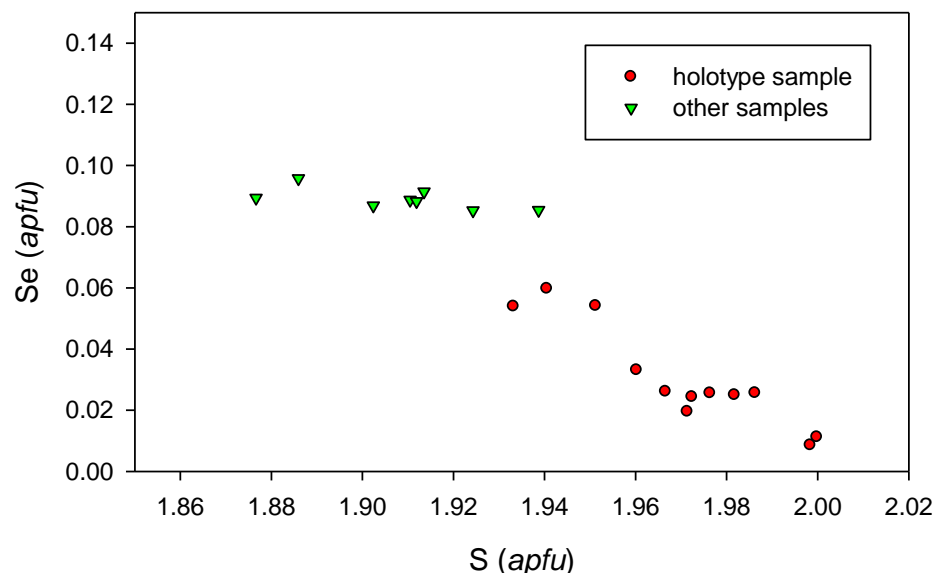


Figure 4. The extent of SeS_{-1} substitution in radvaniceite from Radvanice.

Table 3. Representative chemical analyses for radvaniceite from Radvanice.

		Holotype						Other Samples					
		1	2	3	4	5	6	1	2	3	4	5	6
wt. %	Ge	51.36	52.21	51.23	52.06	51.45	51.73	51.03	52.11	51.25	51.56	51.62	52.08
	Pb	0.28	0.00	0.00	0.45	0.42	0.16	0.00	0.00	0.00	0.00	0.00	0.00
	Sn	0.19	0.00	0.22	0.00	1.23	0.00	0.00	0.00	0.00	0.00	0.00	0.00
	Bi	0.79	0.75	0.54	0.20	1.00	0.56	0.00	0.00	0.00	0.00	0.00	0.00
	Sb	0.25	0.56	0.22	0.00	0.00	0.16	0.00	0.00	0.00	0.00	0.00	0.00
	As	0.38	0.00	0.00	0.28	0.00	0.00	0.00	0.00	0.00	0.00	0.00	0.00
	S	46.54	45.56	45.54	46.66	44.42	45.12	43.79	43.32	43.21	43.54	43.85	42.60
	Se	0.49	1.11	1.41	1.48	3.05	3.08	4.78	4.88	4.95	4.95	5.16	5.33
	total	100.28	100.19	99.16	101.13	101.57	100.81	99.61	100.31	99.40	100.05	100.63	100.00

Table 3. Cont.

		Holotype						Other Samples					
		1	2	3	4	5	6	1	2	3	4	5	6
<i>apfu</i>	Ge	0.97	1.00	0.98	0.98	0.99	0.99	0.99	1.01	1.00	1.00	0.99	1.02
	Pb	0.002	0.000	0.000	0.003	0.003	0.001	0.000	0.000	0.000	0.000	0.000	0.000
	Sn	0.002	0.000	0.003	0.000	0.014	0.000	0.000	0.000	0.000	0.000	0.000	0.000
	Bi	0.005	0.005	0.004	0.001	0.007	0.004	0.000	0.000	0.000	0.000	0.000	0.000
	Sb	0.003	0.006	0.003	0.000	0.000	0.002	0.000	0.000	0.000	0.000	0.000	0.000
	As	0.007	0.000	0.000	0.005	0.000	0.000	0.000	0.000	0.000	0.000	0.000	0.000
Σ		0.993	1.009	0.993	0.988	1.013	0.995	0.990	1.011	1.001	1.000	0.995	1.018
S		1.998	1.971	1.982	1.986	1.933	1.951	1.924	1.902	1.910	1.912	1.914	1.886
Se		0.009	0.020	0.025	0.026	0.054	0.054	0.085	0.087	0.089	0.088	0.091	0.096
Σ		2.007	1.991	2.007	2.012	1.987	2.005	2.010	1.989	1.999	2.000	2.005	1.982

Coefficients of empirical formula calculated on the basis of 3 *apfu*.

5. Raman Spectroscopy

The Raman spectra of radvaniceite were collected in the range of 36–1800 cm^{-1} using a DXR dispersive Raman Spectrometer (Thermo Scientific, Waltham, MA, USA) mounted on a confocal Olympus microscope. The Raman signal was excited by an unpolarised green 532 nm solid state, diode-pumped laser, and detected by a CCD detector. The experimental parameters were: 100 \times objective, 10 s exposure time, 100 exposures, 50 μm pinhole spectrograph aperture and 1 mW laser power level. Eventual thermal damage of the measured points was excluded by visual inspection of excited surfaces after measurement, by observation of possible decay of spectral features at the start of excitation, and by checking for thermal downshift of Raman lines. The instrument was set up by a software-controlled calibration procedure using multiple neon emission lines (wavelength calibration), multiple polystyrene Raman bands (laser frequency calibration) and standardised white-light sources (intensity calibration). Spectral manipulations were performed using Omnic 9 software (Thermo Scientific).

The Raman spectrum of radvaniceite is given in Figure 5, the main bands observed are (in wavenumbers): 437, 411, 374, 343, 311, 281, 262, 204, 182, 175, 138, 131, 105, and 51 cm^{-1} . The experimental spectrum agrees very well with published Raman spectra of synthetic low-temperature β -GeS₂ (e.g., Inoue et al. [29]; Černošek et al. [30]), and distinctly differs from data for high-temperature α -GeS₂ (e.g., Popović [31]; Popović et al. [32]; Inoue et al. [29]; Černošek et al. [30]; Jakšić [33]). According to Bletskan et al. [4], the intramolecular vibrations of the GeS₄ tetrahedra can be described by irreducible representations of the T_d factor-group as follows: $\Gamma_{\text{in}} = A_1 + E + 2F_2$. The A_1 representation corresponds to symmetric stretching vibration ν_1 (Ge-S). The F_2 representation is constituted by antisymmetric stretching ν_3 (Ge-S) and antisymmetric bending ν_4 (S-Ge-S) vibrations, both triply degenerated. Double degenerated E representation describes symmetric bending ν_2 vibration. For the “free” GeS₄ group, wavenumbers of vibrations (all Raman active) are as follows: $\nu_3 = 417$, $\nu_1 = 386$, $\nu_4 = 205$ and $\nu_2 = 170$ cm^{-1} [34]. As a result of GeS₄ tetrahedra deformation in the crystalline field, the degenerated vibrations may be split into two (ν_2) or three components (ν_3 , ν_4). Observed bands in the range 450–250 cm^{-1} are attributed to symmetric (ν_1) and antisymmetric (ν_3) stretching vibrations of corner-sharing GeS₄ tetrahedra; the most intensive band at 343 cm^{-1} is probably connected with ν_1 symmetric stretching vibration [29]. The low intensity bands in the range 250–150 cm^{-1} are attributed to antisymmetric bending ν_4 and symmetric bending ν_2 vibrations. The bands below 150 cm^{-1} should correspond to the external vibrations.

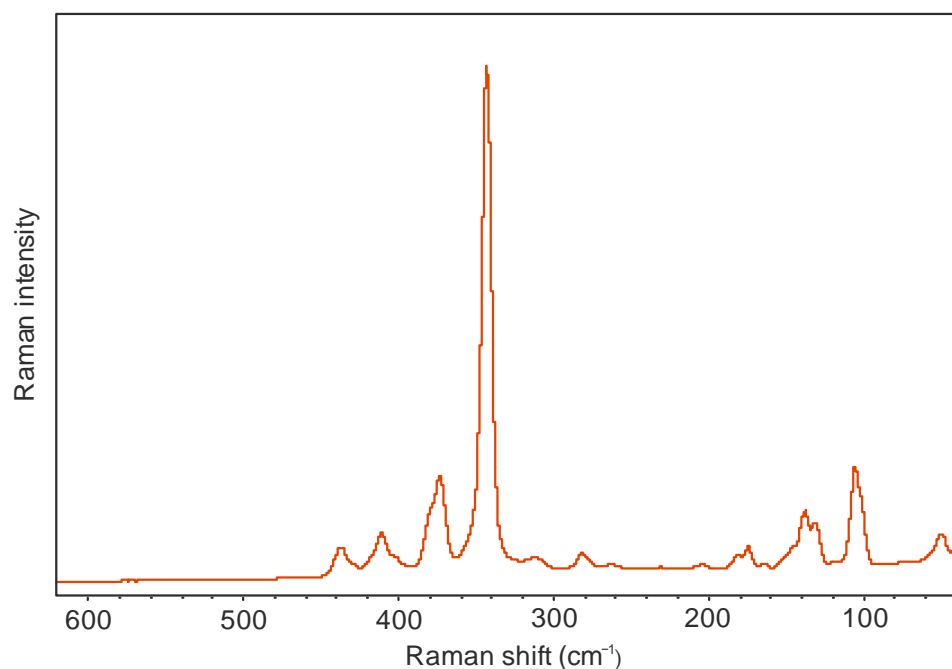


Figure 5. Raman spectrum of radvaniceite in the range 620–36 cm^{-1} .

6. Powder X-ray Diffraction and Crystal Structure

Attempts to obtain single-crystal X-ray data of radvaniceite were unsuccessful due to the nature of the studied material, which is formed by bent fibres (Figure 2).

The X-ray powder diffraction data for radvaniceite (Table 4) were recorded at room temperature using a Bruker D8 Advance diffractometer equipped with a solid-state Lynx-Eye detector and secondary monochromator producing $\text{CuK}\alpha$ radiation, housed at the Department of Mineralogy and Petrology, National Museum, Prague, Czech Republic. The instrument was operated at 40 kV and 40 mA. In order to minimise the background, the powder samples were placed (without any liquid) on the surface of a flat silicon wafer. The powder pattern was collected in the Bragg–Brentano geometry in the range $3\text{--}70^\circ 2\theta$, step 0.01° and counting time of 20 s per step (total duration of the experiment was c. 30 h). The positions and intensities of diffractions were found and refined using the Pearson VII profile-shape function of the ZDS program package [35].

Table 4. X-ray powder diffraction data (d in \AA) for radvaniceite, the strongest diffractions are reported in bold.

I_{meas}	d_{meas}	d_{calc}	I_{calc}^*	h	k	l	I_{meas}	d_{meas}	d_{calc}	I_{calc}^*	h	k	l
100.0	5.7395	{ 5.7422	100	1	1	−1	3.3	2.3028	{ 2.3042	6	1	9	0
7.7	5.6243	{ 5.7422	97	1	1	0			{ 2.3042	6	1	9	−1
15.9	5.2067	{ 5.6252	27	0	4	0	9.5	2.2409	{ 2.2406	5	3	1	−1
		{ 5.2071	29	0	2	1			{ 2.2406	5	3	1	−2
9.1	4.6547	{ 4.6560	11	1	3	−1	3.7	2.1914	{ 2.1913	7	2	2	1
0.9	4.0658	{ 4.6560	11	1	3	0			{ 2.1913	6	2	2	−3
7.3	3.5891	{ 3.5867	19	1	5	0	4.2	2.1326	{ 2.1319	7	1	3	2
		{ 3.5867	21	1	5	−1			{ 2.1319	7	1	3	−3
32.5	3.3650	{ 3.3655	18	1	1	1	7.4	2.0153	{ 2.0150	4	1	9	−2
		{ 3.3655	17	1	1	−2			{ 2.0150	4	1	9	1
6.2	3.0996	{ 3.0995	17	1	3	1	10.9	1.9932	{ 1.9936	11	1	5	2
		{ 3.0995	15	1	3	−2			{ 1.9936	11	1	5	−3
							3.0	1.9296	{ 1.9291	5	0	2	3

Table 4. Cont.

I_{meas}	d_{meas}	d_{calc}	I_{calc}^*	h	k	l	I_{meas}	d_{meas}	d_{calc}	I_{calc}^*	h	k	l
11.6	2.9707	{ 2.9694	6	2	0	0	3.3	1.9134	{ 1.9141	8	3	3	0
		2.9694	5	2	0	−2			1.9141	8	3	3	−3
9.9	2.9365	2.9371	5	0	0	2	3.5	1.8453	{ 1.8443	10	3	7	−1
		2.8711	12	2	2	0			1.8443	9	3	7	−2
8.3	2.8702	{ 2.8711	11	2	2	−2	3.0	1.8116	{ 1.8120	7	3	5	0
		2.8418	17	0	2	2			1.8120	7	3	5	−3
32.9	2.8417	{ 2.8269	21	1	7	0	5.7	1.7865	1.7863	11	0	12	1
		2.8269	21	1	7	−1	5.6	1.7216	1.7208	6	4	0	−2
15.9	2.8236	{ 2.8126	28	0	8	0	12.6	1.6828	{ 1.6827	11	2	2	2
		2.6260	14	2	4	0			1.6827	12	2	2	−4
19.0	2.6257	{ 2.6260	14	2	4	−2	5.0	1.6624	{ 1.6617	8	1	13	0
		2.6036	23	0	4	2			1.6617	8	1	13	−1
9.4	2.6040	2.5356	26	2	6	−1	3.0	1.6454	1.6455	7	4	4	−2
11.3	2.5340	{ 2.3280	6	2	6	0	4.9	1.6262	{ 1.6263	4	1	1	3
		2.3280	6	2	6	−2			1.6263	4	1	1	−4

I_{calc}^* —intensities were calculated using the software PowderCell 2.3 [36] on the basis of the crystal structure of β -GeS₂ [6].

The PXRD data of radvaniceite agree well with the theoretical pattern calculated by the PowderCell 2.3 program [36] from the crystal structure information published by Dittmar and Schäfer [6] for β -GeS₂; this calculated pattern was also used for indexing of experimental data. The following unit-cell parameters, refined by the least-squares program of Burnham [37]: $a = 6.8831(12)$, $b = 22.501(3)$, $c = 6.8081(11)$ Å, $\beta = 120.365(9)^\circ$, $V = 909.8(4)$ Å³ and $Z = 12$, agree very well with data published by Dittmar and Schäfer [6] for β -GeS₂.

Crystal structure of low-temperature β -GeS₂ was published by Zachariasen [7] in orthorhombic symmetry (space group $Fdd2$) with $a = 11.60$ (5), $b = 22.34$ (10), $c = 6.86$ (3) Å; later it was re-determined by Dittmar and Schäfer [6]. In contrast to an earlier determination, they found that it crystallises in the monoclinic space group Pc with unit-cell parameters $a = 6.875$ (5), $b = 22.55$ (1), $c = 6.809$ (5) Å and $\beta = 120.45$ (5)^o. The crystal structure of radvaniceite is based on corner-sharing GeS₄ tetrahedra. In this structure, a system of chains of corner-sharing GeS₄ tetrahedra running along [001] and [010] can be visualised. However, these chains are interconnected by corner-sharing of GeS₄ tetrahedra, forming a framework structure (Figure 6). From a crystallographic point of view, the GeS₄ corner-sharing framework in the radvaniceite crystal structure shows certain similarities to those found in tetrahedral networks of common SiO₂ polymorphs. The main difference lies in the angles of Ge-S-Ge and Si-O-Si bonds connecting two adjacent tetrahedra. In β -GeS₂, an analogue of radvaniceite, this angle varies from 99.8 to 102.8^o whereas in, e.g., α -quartz it has a value of 144^o [38]. Another remarkable feature is that the GeS₄ tetrahedra in the radvaniceite structure are more distorted than corresponding SiO₄ tetrahedra in the α -quartz structure. Whereas the value of quadratic elongation for SiO₄ tetrahedra in α -quartz is 1.0002, values for GeS₄ tetrahedra in the radvaniceite structure fall within the range of 1.008–1.0099.

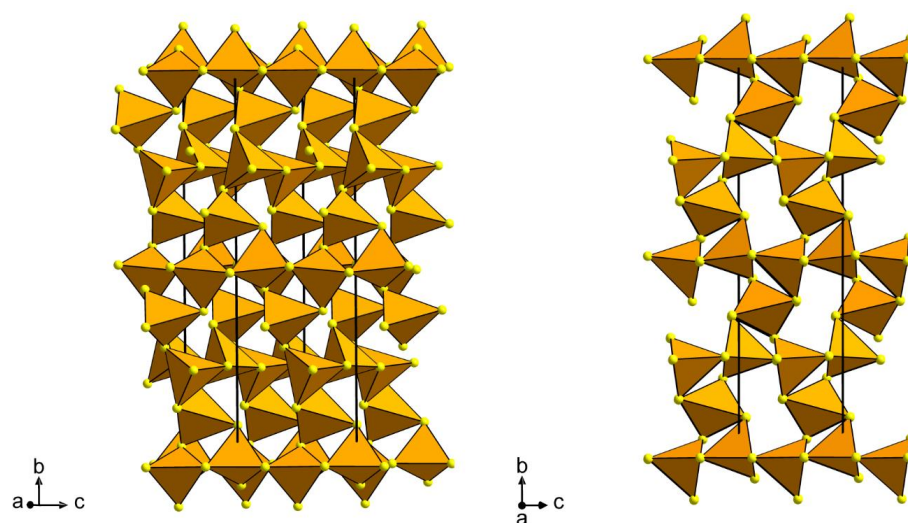


Figure 6. Two views of the crystal structure of radvaniceite showing corner-sharing GeS_4 tetrahedra. Note the chains of GeS_4 tetrahedra running along the [010] and [001] directions (based on the data for $\beta\text{-GeS}_2$ [6]).

7. Note on the Origin of Radvaniceite

The element germanium is compatible with rock-forming silicates, where it substitutes for Si due to its similar ionic radius (0.53 and 0.40 Å, for Si and Ge, respectively) and its possession of the same charge. The bulk Ge content in common rocks varies from ~0.1 to ~2.5 ppm [39,40]. However, Ge can accumulate substantially in some sphalerite deposits, coal, organic matter, and petrified wood [39,40]. As coal from the Radvanice area is substantially enriched in Ge (average 192 g/t, maximum 940 g/t in ash [41]), its spontaneous combustion in the Radvanice dump mobilised Ge and other elements (Sn, Sb, As, Bi, etc.) into escaping hot gases using Cl as a transporting agent (e.g., Laufek et al. [23]) together with omnipresent S and NH_3 . Radvaniceite locally crystallised when the temperature of such mineralised gasses dropped below the stability of the Ge gaseous complexes.

Author Contributions: Conceptualization, J.S. and V.Ž.; methodology, J.S., R.Š., and F.L.; investigation, J.S., R.Š., F.L., and Z.D.; resources, V.Ž. and R.Š.; writing—original draft preparation, J.S. and F.L.; writing—review and editing, J.S. All authors have read and agreed to the published version of the manuscript.

Funding: The research was financially supported by the Ministry of Culture of the Czech Republic (long-term project DKRVO 2019–2023/1.II.d; National Museum, 00023272). The article was also contributed to by the Strategic Research Plan of the Czech Geological Survey (DKRVO/ČGS 2018–2022, Project No 321183).

Data Availability Statement: All representative data are contained in this work.

Acknowledgments: Anonymous referees as well as academic editors Irina O. Galuskina, Igor V. Pekov and Luca Bindi are acknowledged for comments and suggestions that helped to improve the early version of the manuscript.

Conflicts of Interest: The authors declare no conflict of interest.

References

1. MacLachlan, M.J.; Petrov, S.; Bedard, R.L.; Manners, I.; Ozin, G.A. Synthesis and crystal structure of $\delta\text{-GeS}_2$, the first germanium sulfide with an expanded framework structure. *Angewand. Chem. Int. Ed.* **1998**, *37*, 2075–2079. [[CrossRef](#)]
2. Viaene, W.; Moh, G.H. Das binare System Germanium-Schwefel und pT Relation im Druckbereich bis 5 kb. *J. Miner. Abh.* **1973**, *119*, 113–144.
3. Dittmar, G.; Schäfer, H. Die Kristallstruktur von HT- GeS_2 . *Acta Crystallogr.* **1975**, *B31*, 2060–2064. [[CrossRef](#)]
4. Bletskan, D.I.; Kabacij, V.N.; Sakal, T.A.; Stefanovych, V.A. Structure and vibrational spectra of $\text{M}^{\text{II}}\text{A}^{\text{IV}}\text{B}_3^{\text{VI}}$ -type crystalline and glassy semiconductors. *J. Non-Cryst. Solids* **2003**, *326*, 77–82. [[CrossRef](#)]

5. Bletskan, D.I. Phase equilibrium in binary systems $A^{IV}-B^{VI}$. Part. II Systems Germanium-Chalcogen. *J. Ovonic Res.* **2005**, *1*, 47–52.
6. Dittmar, G.; Schäfer, H. Die Kristallstruktur von $LT-GeS_2$. *Acta Crystallogr.* **1976**, *B32*, 1188–1192. [[CrossRef](#)]
7. Zachariasen, W.H. The crystal structure of germanium disulphide. *J. Chem. Phys.* **1936**, *4*, 618–619. [[CrossRef](#)]
8. Wang, N.; Horn, E.E. $\beta-GeS_2$, synthesis and crystal data. *Neues Jahrb. Mineral.* **1975**, 41–44.
9. Málek, J. The thermal stability of chalcogenide glasses. *J. Therm. Anal. Calorim.* **1993**, *40*, 159–170. [[CrossRef](#)]
10. Prewitt, C.T.; Young, H.S. Germanium and silicon disulfides: Structure and synthesis. *Science* **1965**, *149*, 535–537. [[CrossRef](#)]
11. Wang, N.; Horn, E.E. Synthesis and crystal data of a high pressure modification of GeS_2 . *Neues Jahrb. Mineral.-Mon.* **1973**, 413–416. [[CrossRef](#)]
12. Finkelman, R.B.; Larson, R.R.; Dwornik, E.J. Naturally occurring vapor-liquid-solid (VLS) whisker growth of germanium sulfide. *J. Cryst. Growth* **1974**, *22*, 159–160. [[CrossRef](#)]
13. Lapham, D.M.; Barnes, J.H.; Downey, W.F.; Finkelman, R. *Mineralogy Associated with Burning Anthracite Deposits of Eastern Pennsylvania*; Mineral Resource Report 78; Pennsylvania Geological Survey: Harrisburg, PA, USA, 1980; 82p.
14. Sejkora, J.; Berlepsch, P.; Makovicky, E.; Balić-Zunić, T. Natural $SnGeS_3$ from Radvanice near Trutnov (Czech Republic): Its description, crystal structure refinement and solid solution with $PbGeS_3$. *Eur. J. Mineral.* **2001**, *13*, 791–800. [[CrossRef](#)]
15. Sejkora, J. Mineral Association of the Burning Coal Mine Dump of the Kateřina Mine at Radvanice near Trutnov and Processes of Its Origin. Ph.D. Thesis, Faculty of Science, Masaryk University, Brno, Czech Republic, 2002; pp. 1–144. (In Czech)
16. Nickel, E.H.; Grice, J.D. The IMA Commission on New Minerals and Mineral Names: Procedures and guidelines on mineral nomenclature. *Mineral. Petrol.* **1998**, *64*, 237–263. [[CrossRef](#)]
17. Miyawaki, R.; Hatert, F.; Pasero, M.; Mills, S.J. IMA Commission on New Minerals, Nomenclature and Classification (CNMNC), NEWSLETTER 50 New minerals and nomenclature modifications approved in 2019. *Mineral. Mag.* **2019**, *83*, 615–620. [[CrossRef](#)]
18. Žáček, V.; Ondruš, P. Mineralogy of recently formed sublimates from Kateřina colliery in Radvanice, Eastern Bohemia. Czech Republic. *Bull. Czech Geol. Surv.* **1997**, *72*, 289–302.
19. Tvrdý, J.; Sejkora, J. The burning coal mine dump and redeposition of toxic compounds during spontaneous thermic decomposition of coal matter. *EKO—Ekol. A Společnost* **1999**, *10*, 11–15. (In Czech)
20. Sejkora, J.; Makovicky, E.; Balić-Zunić, T.; Berlepsch, P. Stangersite, a new tin germanium sulfide, from the Kateřina mine, Radvanice near Trutnov, Czech Republic. *J. Geosci.* **2020**, *65*, 141–152. [[CrossRef](#)]
21. Žáček, V.; Skála, R. Mineralogy of Burning-Coal Waste Piles in Collieries of the Czech Republic. In *Coal and Peat Fires: A Global Perspective, Volume 3 Case Studies-Coal Fires*; Stracher, G.B., Prakash, A., Sokol, E.V., Eds.; Elsevier: Amsterdam, The Netherlands, 2015; pp. 109–159.
22. Osner, Z.; Němec, J. Remediation of the Burning Waste Bank of the Mine Kateřina (Radvanice, Bohemia). Energie Kladno Ltd. 2002. Available online: http://slon.diamo.cz/hpvt/2002/sekce/zahlazovani/Z11/P_11.htm (accessed on 9 March 2020). (In Czech)
23. Laufek, F.; Veselovský, F.; Drábek, M.; Kříbek, B.; Klementová, M. Experimental formation of Pb, Sn, Ge and Sb sulfides, selenides and chlorides in the presence of sal ammoniac: A contribution to the understanding of the mineral formation processes in coal wastes self-ignition. *Int. J. Coal Geol.* **2017**, *176–177*, 1–7. [[CrossRef](#)]
24. Tásler, R.; Čadková, Z.; Dvořák, J.; Fediuk, F.; Chaloupský, J.; Jetel, J.; Kaiserová-Kalibová, M.; Prouza, V.; Schovánková-Hrdličková, D.; Středa, J.; et al. *Geology of Czech part of the Intra-Sudetic Basin*; Academia: Praha, Czech Republic, 1979; pp. 1–292. (In Czech)
25. Kudělásek, V. Trace elements of coal of the Intra-Sudetic Basin. Part I. *Sbor. Věd. Prac. Vys. Šk. Báň. Ostrava, Ř. Horn.-Geol.* **1959**, *5*, 319–347. (In Czech)
26. Kudělásek, V. Trace elements of coal of the Intra-Sudetic Basin. Part II. *Sbor. Věd. Prac. Vys. šk. Báň. Ostrava, Ř. Horn.-geol.* **1959**, *5*, 457–479. (In Czech)
27. Čadková, Z. The metal distribution in sediments of the Radvanice measures. *Čas. mineral. geol.* **1971**, *16*, 147–157. (In Czech)
28. Pouchou, J.L.; Pichoir, F. “PAP” (ρZ) procedure for improved quantitative microanalysis. In *Microbeam Analysis*; Armstrong, J.T., Ed.; San Francisco Press: San Francisco, CA, USA, 1985; pp. 104–106.
29. Inoue, K.; Matsuda, O.; Murase, K. Raman spectra of tetrahedral vibrations in crystalline germanium dichalcogenides, GeS_2 and $GeSe_2$, in high and low temperature forms. *Solid Stat. Comm.* **1991**, *79*, 905–910. [[CrossRef](#)]
30. Černošek, Z.; Černošková, E.; Beneš, L. Raman scattering in GeS_2 glass and its crystalline polymorphs compared. *J. Mol. Struct.* **1997**, *435*, 193–198. [[CrossRef](#)]
31. Popović, Z.V. Molecular vibration in $Sn(Pb)GeS_3$ and GeS_2 . *Phys. Lett.* **1983**, *A94*, 242–246. [[CrossRef](#)]
32. Popović, Z.V.; Holtz, M.; Reimann, K.; Syassen, K. High-pressure Raman scattering and optical absorption study of $\beta-GeS_2$. *Phys. Stat. Solid.* **1996**, *198*, 533–537. [[CrossRef](#)]
33. Jakšić, Z.M. Temperature and pressure dependence of phonon frequencies in GeS_2 , $GeSe_2$, and $SnGeS_3$. *Phys. Stat. Solid.* **2003**, *239*, 131–143. [[CrossRef](#)]
34. Pohl, S.; Schiwiy, W.; Weinstock, N.; Krebs, B. Darstellung, Schwingungsspektren und Normalkoordinatenanalyse der Ionen GeS_4^{4-} und SnS_4^{4-} . *Z. Naturforsch.* **1973**, *B28*, 565–569. [[CrossRef](#)]
35. Ondruš, P. A computer program for analysis of X-ray powder diffraction patterns. *Mater. Sci. Forum EPDIC-2 Enchede* **1993**, 133–136, 297–300. [[CrossRef](#)]
36. Kraus, W.; Nolze, G. POWDER CELL—A program for the representation and manipulation of crystal structures and calculation of the resulting X-ray powder patterns. *J. Appl. Crystallogr.* **1996**, *29*, 301–303. [[CrossRef](#)]

37. Burnham, C.W. Lattice constant refinement. *Carnegie Inst. Wash. Yearb.* **1962**, *61*, 132–135.
38. Le Page, Y.; Donnay, G. Refinement of the crystal structure of low-quartz. *Acta Crystallogr.* **1976**, *B32*, 2456–2459. [[CrossRef](#)]
39. Bernstein, L.R. Germanium geochemistry and mineralogy. *Geochim. Cosmochim. Acta* **1985**, *49*, 2409–2422. [[CrossRef](#)]
40. Höll, R.; Kling, M.; Schroll, E. Metallogenesis of germanium—A review. *Ore Geol. Rev.* **2007**, *30*, 145–180. [[CrossRef](#)]
41. Pešek, J.; Sýkorová, I.; Jelínek, E.; Michna, O.; Forstová, J.; Martínek, K.; Vašíček, M.; Havelcová, M. Major and minor elements in the hard coal from the Czech Upper Paleozoic basins. *Czech Geol. Surv. Spec. Pap.* **2010**, *10*, 1–48.